ORGANIC LETTERS

2012
Vol. 14, No. 17
4434–4437

Relative Configuration of JBIR-129, a Cytotoxic 34-Membered Glycosidic Polyol Macrolide from *Streptomyces* sp. RK74

Teppei Kawahara,[†] Miho Izumikawa,[†] Motoki Takagi,[†] and Kazuo Shin-ya*[,‡]

Japan Biological Informatics Consortium (JBIC), 2-4-7 Aomi, Koto-ku, Tokyo 135-0064, Japan, and National Institute of Advanced Industrial Science and Technology (AIST), 2-4-7 Aomi, Koto-ku, Tokyo 135-0064, Japan

k-shinya@aist.go.jp

Received July 13, 2012

ABSTRACT

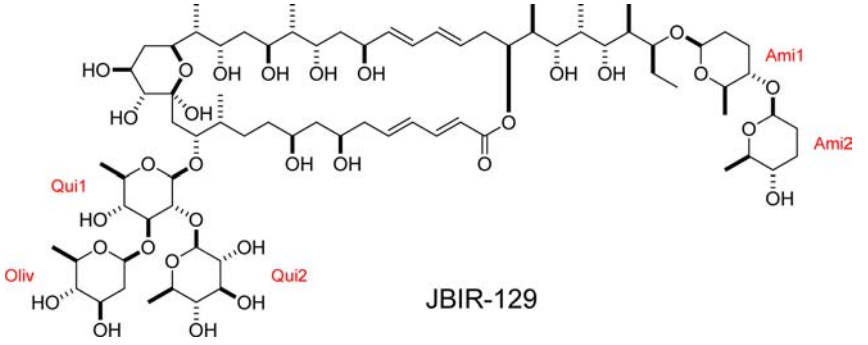

JBIR-129 was isolated as the potent cytotoxic compound, which consists of the 34-membered polyol macrolide skeleton with five sugar moieties. The relative configuration of the aglycone moiety (C7−C27 and C33−C39) was established by the *J*-based configuration analysis using vicinal $^{1}H-^{1}H$ (from ^{1}H NMR and PS-DQF-COSY spectra) and long-range $^{1}H-^{13}C$ coupling constants (from sge-HETLOC and several *J*-resolved HMBC spectra) with steric information obtained from ROESY.

JBIR-129 (**1**) and its congener (JBIR-139), the GalNAc adduct at C-21, were isolated from *Streptomyces* sp. RK74 as the potent cytotoxic compounds against human ovarian adenocarcinoma SKOV-3 cells with IC_{50} values of 0.3 and 0.4 μM, respectively. We have described the discovery, fermentation, isolation, structure elucidation including relative configuration of sugar units, and preliminary biological activities of **1** and JBIR-139.[1] In previous studies, the stereochemistry of large-ring macrolides (>16 ring atoms) have been determined by using steric information (NOE or ROE) and X-ray crystallography combined with application of chemical modifications such as fragmentation. However, it is not usually desirable to elucidate the structures of natural compounds by chemical degradation, especially when their recoveries are small. The *J*-based configuration analysis (JBCA)[2] method has been widely applied to the elucidation of the relative configurations of various compounds.[3−5] Although JBCA is mainly used for acyclic compounds, some fragments of large-ring macrolides are considered to have sufficiently flexible molecular structures. In fact, relative

[†] JBIC.
[‡] AIST.

(1) Kawahara, T.; Hwang, J.-H.; Izumikawa, M.; Hashimoto, J.; Takagi, M.; Shin-ya, K. *J. Nat. Prod.* Submitted.

(2) Matsumori, N.; Kaneno, D.; Murata, M.; Nakamura, H.; Tachibana, K. *J. Org. Chem.* **1999**, *64*, 866–876.

(3) (a) Huang, S.-X.; Wang, X.-J.; Yan, Y.; Wang, J.-D.; Zhang, J.; Liu, C.-X.; Xiang, W.-S.; Shen, B. *Org. Lett.* **2012**, *14*, 1254–1257. (b) Wu, M.; Okino, T.; Nogle, L. M.; Marquez, B. L.; Williamson, R. T.; Sitachitta, N.; Berman, F. W.; Murray, T. F.; McGough, K.; Jacobs, R.; Colsen, K.; Asano, T.; Yokokawa, F.; Shioiri, T.; Gerwick, W. H. *J. Am. Chem. Soc.* **2000**, *122*, 12041–12042. (c) Kobayashi, H.; Shin-ya, K.; Furihata, K.; Hayakawa, Y.; Seto, H. *Tetrahedron Lett.* **2001**, *42*, 4021–4023. (d) Sugahara, K.; Kitamura, Y.; Murata, M.; Satake, M.; Tachibana, K. *J. Org. Chem.* **2011**, *76*, 3131–3138.

(4) (a) Bedke, D. K.; Shibuya, G. M.; Pereira, A.; Gerwick, W. H.; Haines, T. H.; Vanderwal, C. D. *J. Am. Chem. Soc.* **2009**, *131*, 7570–7572. (b) Kawahara, T.; Kumaki, Y.; Kamada, T.; Ishii, T.; Okino, T. *J. Org. Chem.* **2009**, *74*, 6016–6024.

(5) Ardá, A.; Rodríguez, J.; Nieto, R. M.; Bassarello, C.; Gomez-Paloma, L.; Bifulco, G.; Jiménez, C. *Tetrahedron* **2005**, *61*, 10093–10098.

10.1021/ol301940q
Published on Web 08/21/2012

configurations of medium- and large-ring macrolides have been elucidated using JBCA.[6] Therefore, we have applied the JBCA method to determine the relative stereochemistry of the aglycone of **1**. However, overlapping of the ^{1}H NMR signals, which results from the high degree of oxygenation, complicates the application of this strategy to **1**. Thus, we carefully determined $^{3}J_{H,H}$, $^{2}J_{C,H}$, and $^{3}J_{C,H}$ values using a combination of phase-sensitive double-quantum-filtered (PS-DQF)-COSY, exclusive correlation spectroscopy (E-COSY), sensitivity- and gradient-enhanced hetero (ω_1) half-filtered TOCSY (sge-HETLOC),[7] and several *J*-resolved HMBC[8,9] spectral analyses.

JBIR-129 (**1**) was isolated as a colorless amorphous solid from the culture broth of *Streptomyces* sp. RK74 by bioassay-guided fractionation using various chromatographic purifications.[1] The planar structure of **1** has already been established from the analyses of UV, IR, HR-ESI-TOFMS, and 1D and 2D NMR spectroscopic data (Figure 1). The relative configurations of five sugar moieties (two β-quinovopyranoside, one β-olivopyranoside, and two β-amicetopyranoside moieties) have also been determined by the corresponding ^{1}H−^{1}H coupling constants and ROESY correlations.

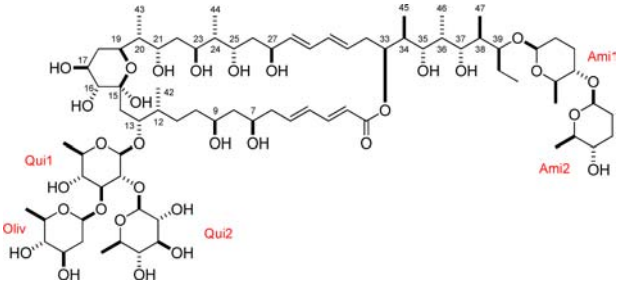

Figure 1. Structure of JBIR-129 (**1**). The relative stereochemistries shown in the C7−C27 and C33−C39 fragments and sugar moieties are independent.

The relative configurations of the three contiguous carbon chain sequences of **1** (C7−C14, C19−C27, and C33−C39) were established by JBCA as follows. First, to utilize JBCA, we needed to obtain more $^{3}J_{H,H}$ values in addition to those from the previous investigation. Therefore, we assigned the detailed corresponding *J* values from the high-resolution PS-DQF-COSY and E-COSY spectra (Table S1 in Supporting Information). Long-range ^{1}H−^{13}C coupling constants were given by sge-HETLOC,[7] *J*-resolved HMBC-1 and -2,[8] and the selective *J*-resolved HMBC[9] spectra. The sge-HETLOC spectrum was effective for the analyses of oxymethine proton NMR regions and indeed provided the majority of the required $^{2,3}J_{C,H}$ (Figure S18). The *J*-resolved HMBC-1 and -2 spectra did not provide further information because of their low signal-to-noise (S/N) ratio. However, on the basis of these HMBC data, we measured the selective *J*-resolved HMBC, and the remaining ^{1}H−^{13}C long-range coupling constants are able to be acquired from the resulted spectra, even from higher multiply coupled protons, which connect with methylene and/or methyl groups at neighbors (Figures S21−24).

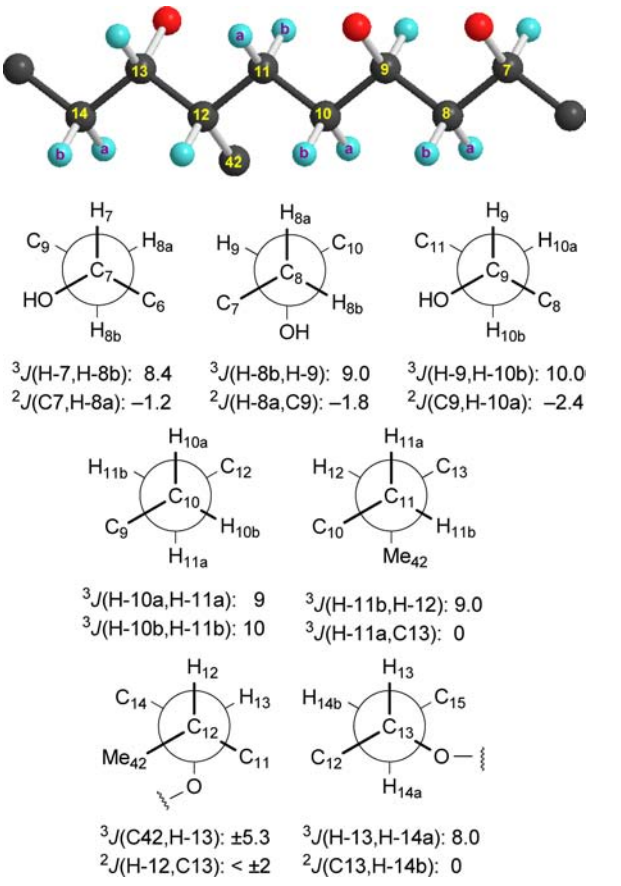

Figure 2. Relative configuration determined for C7−C14; ^{2}J and ^{3}J are in hertz.

At the C7/C8 axis, a large coupling constant between H-7 and H-8b ($^{3}J_{H\text{-}7,H\text{-}8b}$ = 8.4 Hz) inferred the *anti* orientation of H-7/H-8b. A small $^{2}J_{C7,H\text{-}8a}$ value (−1.2 Hz) obtained from the sge-HETLOC spectrum indicated that O-7 and H-8a are in the *anti* orientation (Figure 2). For the C8/C9 bond, the large $^{3}J_{H\text{-}8b,H\text{-}9}$ value (9.0 Hz) was consistent with the *gauche* orientation between C7 and H-9. The *anti* orientation of H-8a/O-9 was deduced from the small value of $^{2}J_{H\text{-}8a,C9}$ (−1.8 Hz). For C9/C10, a large $^{3}J_{H\text{-}9,H\text{-}10b}$ (10.0 Hz) indicated the *anti* orientation between H-9 and H-10b. An additional small $^{2}J_{C9,H\text{-}10a}$ (−2.4 Hz) was indicative of the *anti* orientation between H-10a and O-9.

(6) (a) Williams, P. G.; Miller, E. D.; Asolkar, R. N.; Jensen, P. R.; Fenical, W. *J. Org. Chem.* **2007**, *72*, 5025–5034. (b) Park, H. R.; Chijiwa, S.; Furihata, K.; Hayakawa, Y.; Shin-ya, K. *Org. Lett.* **2007**, *9*, 1457–1460. (c) Umeda, Y.; Furihata, K.; Sakuda, S.; Nagasawa, H.; Ishigami, K.; Watanabe, H.; Izumikawa, M.; Takagi, M.; Doi, T.; Nakao, Y.; Shin-ya, K. *Org. Lett.* **2007**, *9*, 4239–4242.

(7) Uhrín, D.; Batta, G.; Hruby, V. J.; Barlow, P. N.; Kövér, E. *J. Magn. Reson.* **1998**, *130*, 155–161.

(8) Furihata, K.; Seto, H. *Tetrahedron Lett.* **1999**, *40*, 6271–6275.

(9) Furihata, K.; Tashiro, M.; Seto, H. *Magn. Reson. Chem.* **2009**, *47*, 814–818.

It was difficult to obtain the $^1H-^1H$ coupling constants corresponding to the C10/C11 axis from the PS-DQF-COSY spectrum. We sliced the PS-DQF-COSY spectrum at δ_H 3.80 (H-9) to yield $J_{H\text{-}10a} \approx 3$, 3, 9, and 12 Hz and $J_{H\text{-}10b} \approx 3$, 9, 10, and 12 Hz, while the slice at the peak of H-12 (δ_H 2.25) gave $J_{H\text{-}11a} \approx 3$, 3, 9, and 12 Hz and $J_{H\text{-}11b} \approx 3$, 9, 10, and 12 Hz. Additionally, we sliced at the signal at δ_H 1.02 (H-11b) in the PS-DQF-COSY spectrum to yield $^3J_{H\text{-}11b,H\text{-}12} \approx 9$ Hz, $^2J_{H\text{-}11a,H\text{-}11b} \approx 12$ Hz, and $^3J_{H\text{-}10b,H\text{-}11b} \approx 10$ Hz. These results provided the large coupling constants between H-10a and H-11a ($^3J_{H\text{-}10a,H\text{-}11a} \approx 9$ Hz) and between H-10b and H-11b, which established the *anti* relationships between the protons in these pairs. For the C11/C12 moiety, a large $^3J_{H\text{-}11b,H\text{-}12}$ value indicated that H-11b and H-12 are in the *anti* orientation. Furthermore, a small $^3J_{H\text{-}11a,C13}$ (~0 Hz) established that H-11a and C13 were in the *gauche* orientation. At C12/C13, a small $^2J_{H\text{-}12,C13}$ ($< \pm 2$ Hz), obtained from the selective *J*-resolved HMBC measurement, indicated that H-12 and O-13 are in the *anti* orientation. Together with this data, a large $^3J_{C42,H\text{-}13}$ value (± 5.3 Hz) indicated that C42 and H-13 are in the *anti* conformation. For the relationship between C13 and C14, a large $^3J_{H\text{-}13,H\text{-}14a}$ value (8.0 Hz) and a small $^2J_{C13,H\text{-}14b}$ value (~0 Hz) established the *anti* orientations of both H-13/H-14a and H-14b/O-13. Hence, the dominant conformation of the C7–C14 fragment turned out to be in a zigzag conformation, and the relative configurations at C7, C9, C12, and C13 were established as 7*S**, 9*R**, 12*S**, and 13*S**, respectively (Figure 2).

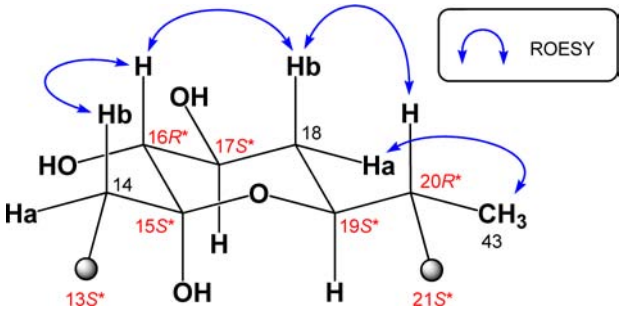

Figure 3. Relative configuration of C13 to C21.

The relative configuration of the tetrahydropyran moiety (C15–C19) was determined from $^1H-^1H$ coupling constants and ROESY correlations.[10] Large coupling constants $^3J_{H\text{-}16,H\text{-}17}$ (9.0 Hz), $^3J_{H\text{-}17,H\text{-}18b}$ (11.5 Hz), and $^3J_{H\text{-}18b,H\text{-}19}$ (10.2 Hz) indicated that they are in diaxial orientations. The small coupling constant between H-17 and H-18a ($^3J_{H,H} = 4.0$ Hz) also supported the relative configuration of this moiety. In the ROESY spectrum, cross-couplings among H-14b (δ_H 1.54), H-16 (δ_H 3.40), H-18b (δ_H 1.25), and H-20 (δ_H 1.44) were observed, which proved that the tetrahydropyran ring moiety is in the chair conformation. Therefore, O-15 and H-16 were in *anti* orientation. Hence, the relative configuration of the tetrahydropyran moiety was deduced as 15*S**, 16*R**, 17*S**, and 19*S** (Figure 3).

For the C19–C20 axis, the observation of a large $^3J_{H\text{-}19,H\text{-}20}$ value (7.2 Hz) indicated that H-19 and H-20 are in the *anti* orientation. The relative configuration at C20 was established to be *R** according to the ROE between H-43 and H-18a (Figure 4). For the C20/C21 bond, the relationship of C43/H-21 was revealed as *anti* based on a large $^3J_{C43,H\text{-}21}$ value (± 5.4 Hz). A small value of coupling constant $^2J_{H\text{-}20,C21}$ ($< \pm 2$ Hz) led us to determine that the relative configuration at C21 is *S**. For the C21/C22 bond, the observation of a large $^3J_{H\text{-}21,H\text{-}22a}$ value (11.1 Hz) established that H-21 and H-22a are in the *anti* orientation.

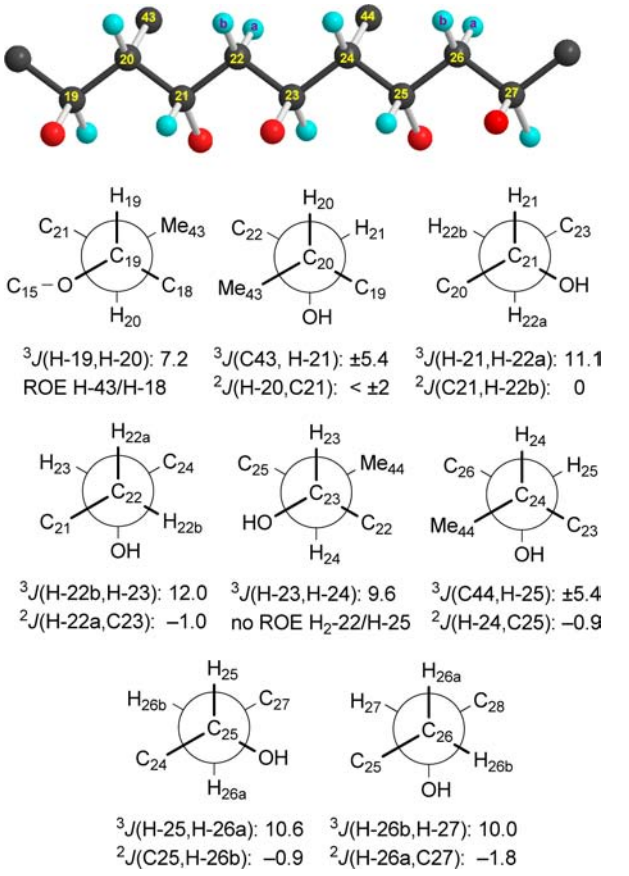

Figure 4. Relative configuration determined for C19 to C27; ^2J and ^3J are in hertz.

From the small value of $^2J_{C21,H\text{-}22b}$ (~0 Hz) obtained by analyses of the sge-HETLOC spectrum, it was concluded that O-21 and H-22b are in the *anti* conformation. For C22 and C23, a large $^3J_{H\text{-}22b,H\text{-}23}$ value (12.0 Hz) and a small $^2J_{H\text{-}22a,C23}$ value (−1.0 Hz) revealed that both H-22b/H-23 and H-22a/O-23 are in the *anti* orientation, establishing the relative configuration at C23 as *S**. The relationship between C23 and C24 was elucidated as follows. A large

(10) Kishi, Y. *Pure Appl. Chem.* **1993**, *65*, 771–778.

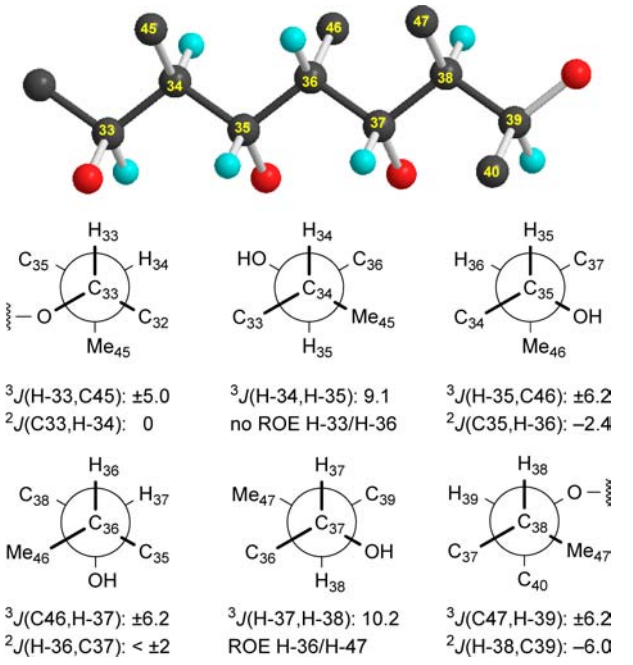

Figure 5. Relative configuration determined for C33 to C39; ^{2}J and ^{3}J are in hertz.

value of $^{3}J_{\text{H-23,H-24}}$ (9.6 Hz) revealed that these protons are in the *anti* orientation. The relative configuration at C-24 was concluded to be *R** by the lack of ROESY correlation between H_2-22 (δ_{Ha} 1.84, δ_{Hb} 1.14) and H-25 (δ_H 4.38). For the C24/C25 bond, a small $^{2}J_{\text{H-24,C25}}$ value (−0.9 Hz) and a large $^{3}J_{\text{C44,H-25}}$ (±5.4 Hz) indicated both H-24/O-25 and C44/H-25 are in the *anti* orientation, which led to the determination of C25 as *S**. For C25−C26, a large $^{3}J_{\text{H-25,H-26a}}$ (10.6 Hz) and a small $^{2}J_{\text{C25,H-26b}}$ (−0.9 Hz) value established the *anti* relationships between both H-25/H-26a and O-25/H-26b. For the C26/C27 axis, a large $^{3}J_{\text{H-26b,H-27}}$ value (10.0 Hz) indicated that these protons are in the *anti* orientation. In addition, a small $^{2}J_{\text{H-26a,C27}}$ value (−1.8 Hz) was observed, proving that H-26a and O-27 are in the *anti* orientation. Therefore, the relative configuration at C-27 was deduced to be *S**, thus completing the relative configurational assignment for the C19 to C27 fragment (Figure 4).

For the C33−C34 bond, a large $^{3}J_{\text{H-33,C45}}$ value (±5.0 Hz) indicated that H-33 and C45 are in the *anti* orientation. A small $^{2}J_{\text{C33,H-34}}$ value (~0 Hz) established that O-33 and H-34 are also in the *anti* orientation. Thus, the relative configurations at C-33 and C-34 were both elucidated to be *S**. A large coupling constant between H-34 and H-35 (9.1 Hz) was indicative that these protons are in the *anti* orientation. The configurations at C35, C36, and C37 were established by large values of $^{3}J_{\text{H-35,C46}}$ (±6.2 Hz) and $^{3}J_{\text{C46,H-37}}$ (±6.2 Hz) and small coupling constants between C35 and H-36 ($^{2}J_{\text{C35,H-36}} = -2.4$ Hz) and H-36 and C37 ($^{2}J_{\text{H-36,C37}} < \pm 2$ Hz) to be 35*S**, 36*R**, and 37*R**, respectively. For C37/C38, *anti* orientation of the protons in this bond was deduced from the large $^{3}J_{\text{H-37,H-38}}$ value (10.2 Hz) obtained from the PS-DQF-COSY spectrum. In the ROESY spectrum, an ROE between H-36 and H-47 (δ_H 0.82) was observed. Taking these data into consideration, the relative configuration at C38 was proved to be *R**. The relative configuration at C39 was determined to be *S** according to large $^{3}J_{C,H}$ and $^{2}J_{C,H}$ values between C47/H-39 ($^{3}J_{\text{C47,H-39}} = \pm 6.2$ Hz) and between H-38/C39 ($^{2}J_{\text{H-38,C39}} = -6.0$ Hz), respectively. Since an ROE between H-33 and H-36 was not observed, the relative configuration for the C33−C39 moiety was deduced as 33*S**, 34*S**, 35*S**, 36*R**, 37*R**, 38*R**, and 39*S**, respectively (Figure 5).

Thus, partial relative configurations of **1** were determined as shown in Figure 1. Further biological activities, biosynthetic studies, and determination of the absolute configuration of **1** are currently under way.

Acknowledgment. The authors are grateful to Dr. Kazuo Furihata at the Division of Agriculture and Agricultural Life Sciences, The University of Tokyo, and Dr. Eri Fukushi of the GC-MS & NMR Laboratory at the Graduate School of Agriculture, Hokkaido University, for helpful discussions. This work was supported in part by a grant from the New Energy and Industrial Technology Development Organization (NEDO) of Japan, a Grant-in-Aid for Scientific Research (23380067 to K.S.) from the Japan Society for the Promotion of Science (JSPS), and a research program of the Project for Development of Innovation Research on Cancer Therapeutics (P-Direct), Ministry of Education, Culture, Sports, Science and Technology of Japan.

Supporting Information Available. General methods, Table S1, HRESIMS spectrum, and assorted 1D and 2D NMR spectra for JBIR-129. This material is available free of charge via the Internet at http://pubs.acs.org.

The authors declare no competing financial interest.